19th International Conference on
Adaptive Structures and Technologies
October 6-9, 2008
Ascona, Switzerland

Speckle Interferometry for Damage Detection in Thin-Walled Adaptive Structures

Rolf Lammering
Institute of Mechanics, Helmut-Schmidt-University / University of the Federal Armed Forces Hamburg,
Hostenhofweg 85, 22043 Hamburg,
Tel.: ++49-40-6541-2734, Fax: ++49-40-6541-2034, E-mail: rolf.lammering@hsu-hh.de

ABSTRACT

Lamb waves have shown to be favorably applicable in the development of health monitoring systems in structural mechanics since they show reflections, refractions, as well as mode conversions at fault locations. For the observation of the wave propagation, the double pulsed electronic speckle pattern interferometry (ESPI) as a high precision, full-field, and non-contact measurement technique is under investigation in this work. It is shown that not only symmetric and antisymmetric waves can be captured but that also various faults in plate structures can be detected. A riveted lightweight structure serves as another test specimen. The location of the rivets is clearly identifiable by this measuring technique.

Keywords: structural health monitoring, Lamb waves, ESPI, speckle interferometry

1. INTRODUCTION

Modern infrastructure includes a vast variety of structural systems which have to be kept under surveillance in order to avoid malfunction and accidents. Typical examples are steel and concrete bridges, pressure vessels, railway vehicles as well as railway tracks, and transmission lines, to name just a few. Especially aerospace structures are in the focus of improved inspection techniques since a considerably amount of life cycle costs is due to inspection and repair and since damage can lead to catastrophic failure. A reliable monitoring technique would allow for adjusting maintenance intervals in accordance to the real requirements so that a reduction of the operating costs is expected. Moreover, the increasing application of fiber reinforced plastics in lightweight aerospace structures is currently demanding for advanced monitoring techniques.

Therefore, the main goal of structural health monitoring methods and non-destructive testing techniques which are currently under research is the fast, efficient, and reliable detection of visible and hidden structural damages in engineering structures.

The difficulty in identifying the damage is often caused by the complex phenomena of damage initiation and evolution including various failure modes which have to be detected reliably. Among others, techniques based on elastic waves play an important role for damage detection. In plate and shell structures, especially high frequency waves, i.e. Lamb waves, and their possible contributions to structural health monitoring methods are in the focus of current research, cf. Giurgiutiu [1]. Reflections, refractions or mode conversions are distinct indications of faults or defects and are often instantaneous visible in the pattern of an otherwise undisturbed propagating wave. Since

interferometric measurement techniques allow for the visualization of wave propagation they are candidate techniques for the detection of fault induced irregularities and thus of structural damage.

The aim of this work is to investigate the potential of speckle interferometry in the observation of Lamb waves and in the detection of faults in thin plate and shell structures. This interferometric measurement technique is based on laser illumination and enables investigations in many fields of applications, e.g. strain and vibration analysis, flow visualization and non-destructive testing. In the case of fault detection the surface displacements of the specimens are observed. The accuracy of this full field measurement technique is at the order of the light wave. However, the application of this measurement technique, especially the double pulsed Electronic Speckle Pattern Interferometry (ESPI), to Lamb wave observation is rare and only a few publications exist to the knowledge of the author, cf. Gordon et al. [2] and Mast et al. [3]. On the other hand, scanning laser vibrometry as an alternative measurement technique is frequently used, cf. e.g. Staszewski et al. [4] or Barth et al. [5].

Beside the observation of Lamb waves their generation in thin plates and shells is an important issue. For that purpose small piezoelectric wafers are integrated into structures or are adhered to their surfaces. They are driven by an electric voltage at high frequencies and are thus able for the generation of Lamb waves. Piezoelectric wavers may also be used as sensors and thus for the detection of Lamb waves at selected locations of the structure under investigation. However, this alternative approach does not provide full-field information in contrast to the optical measurement technique considered in this work. In any case, laborious scanning is avoided and the observation of large areas becomes possible.

The organization of the manuscript is as follows: In the next section a brief introduction into the physics of wave propagation is given with special regard to the characteristics which allow for fault detection. Since the speckle interferometry is applied to observe the surfaces of the specimens optically a brief introduction into this technique is given subsequently. The main part of the manuscript deals with the presentation of experimental results. They are obtained from plate structures without and with artificial faults as well as from the riveted elevator flap of an aircraft. The speckle interferometry has proven to be an appropriate measurement technique for wave propagation observation and fault detection since the Lamb wave could be captured and the faults were successfully identified in the plate specimens. Furthermore, the locations of the rivets were localized clearly.

2. WAVE MOTION IN ELASTIC MEDIA

In the analysis of wave motion in elastic media the Lamé-Navier equations serve as a starting point. These equations may be considered as the local formulation of the balance of momentum in which Hooke's law of an isotropic media has been introduced in order to replace the stresses by displacement derivatives. Thus, the well known equation

$$(\lambda+\mu)u_{j,ji}+\mu u_{i,jj}+\rho f_i=\rho\ddot{u}_i \tag{1}$$

is obtained which may be written alternatively as

$$(\lambda+\mu)\nabla(\nabla\mathbf{u})+\mu\nabla^2\mathbf{u}+\rho\mathbf{f}=\rho\ddot{\mathbf{u}} \tag{2}$$

In equations (1) and (2) λ and μ denote the Lamé constants, u_j respective $\mathbf{u}$ represents the displacement field, ρ is the material density and f_i respective $\mathbf{f}$ the distributed volume specific body forces. In equation (1) an index separated by a comma indicates differentiation with respect to the designated coordinate and a superimposed dot with respect to time. In equation (2) bold quantities denote vectors and ∇ represents the Nabla-operator. Solutions of these coupled, linear differential equations are given in many textbooks, cf. Achenbach [6] or Graff [7].

In the case of an unbounded elastic media it is well known that two and only two types of waves are propagating, namely the compression (P-) wave and the shear (S-) wave. These types of

waves are also fundamental to the following considerations.

In the case of elastic semi-infinite media the existence of a boundary comes into play and distinguishes this problem from the latter. The analysis leads to the phenomenon of mode conversion that occurs when waves encounter a free boundary. This means that in the case of an incident P- or S-wave, both a P-wave as well as an S-wave may be reflected. Similar effects are observed at the interface between two elastic layers. In the analysis of the reflections Snell's law is fundamental. The result of the respective mathematical problem, i.e. differential equations including boundary condition, is interpreted as a surface wave which is a third type of wave. These waves have been named after Lord Rayleigh who showed that their amplitudes decrease rapidly with depth. Depending on Poisson's ratio of the media the velocity of propagation is somewhat less than shear velocity. Rayleigh waves are non-dispersive.

2-1. Lamb waves

Like in the case of the elastic semi-infinite media the Lamé-Navier equations (1) and (2) are solved with respect to the boundary conditions for plate and shell problems. The existence of two parallel free surfaces entails a new type of wave, so-called Lamb waves or guided plate waves. In contrast to the unbounded or semi-infinite elastic media in which only a limited number of waves are able to develop an infinite number of waves may emerge in plates and shells. Their formation may be considered as a consequence of P- and S-wave reflections at the surfaces of plates and shells. Many textbooks, e.g. Graff [7] or Giurgiutiu [1], deal with the Lamb wave theory which is only shortly outlined here for that reason.

For an infinite homogeneous elastic plate of thickness *2d* the x_1-x_2-plane is assumed to coincide with the mid plate surface and its normal with the x_3-direction. Due to the infinite extension in the x_2-direction, this coordinate is of no significance and a plane strain state in the x_1-x_3-plane is analyzed. In contrast to these conditions by which straight crested waves are investigated, a cylindrical coordinate system and the assumption of an axisymmetric stress state allows for the analysis of circular crested waves, cf. von Ende et al. [8]. In the case of the plane strain state and neglected body forces the Lamé-Navier equations (1) and (2) are transferred by use of two potential functions ϕ and ψ into the following equations:

$$\begin{aligned} \phi_{,11} + \phi_{,33} &= \frac{1}{c_L^2}\phi_{,tt} \\ \psi_{,11} + \psi_{,33} &= \frac{1}{c_T^2}\psi_{,tt} \end{aligned} \tag{3}$$

Here, the phase velocity of the pressure (longitudinal) wave is denoted by $c_L = \sqrt{(\lambda + 2\mu)/\rho}$ and the phase velocity of the shear (transverse) wave by $c_T = \sqrt{\mu/\rho}$. The potential functions ϕ and ψ are multiplicatively decomposed in a standing wave in x_3- and a propagating wave in x_1-direction:

$$\begin{aligned} \phi &= \Phi(x_3)\, e^{i(k x_1 - \omega t)} \\ \psi &= \Psi(x_3)\, e^{i(k x_1 - \omega t)} \end{aligned} \tag{4}$$

In these equations, *k* stands for the wave number and ω for the excitation frequency. From ϕ and ψ the displacements are computed by differentiation and subsequently the stresses are analyzed. Taking into account the stress-free boundary conditions at both sides of the plate the Rayleigh-Lamb wave equation is obtained

$$\frac{\tan qd}{\tan pd} = -\left[\frac{4k^2 pq}{\left(q^2 - k^2\right)^2}\right]^{\pm 1} \tag{5}$$

regardless whether straight or circular crested waves are under consideration. The parameters p and q are defined as $p^2 = \omega^2 / c_L^2 - k^2$ and $p^2 = \omega^2 / c_T^2 - k^2$. The numerical solution of equation (5) with the exponent +1 yields the symmetric eigenvalues k_i^S, with consideration of the exponent - 1 the antisymmetric eigenvalues k_i^A are received. Each eigenvalue corresponds to a Lamb wave mode shapes which are designated as S_i and A_i modes dependent on whether they are symmetric or antisymmetric, respectively.

The eigenvalues k_i^S and k_i^A are functions of the excitation frequency since the parameters p and q are depending on the angular frequency ω. The subsequently computed phase velocities $c_i = \omega / k_i$ are also functions of the excitation frequency, indicating the dispersive character of the Lamb waves.

2-1. Characteristics of Lamb waves

From the solution of equation (5) which is graphically shown in Figure 1 one obtains the result that an infinite number of wave modes propagate in plates and shells and that at least two modes exist at any frequency. In structural health monitoring the fundamental symmetric (S_0) and antisymmetric (A_0) modes (see Figure 2) are typically generated without excitation of higher modes. Lamb waves are able to propagate over long distances in thin plate and shell structures with low attenuation so that they are attractive for health monitoring techniques. Due to their short wavelength they are also applicable for the detection of small faults.

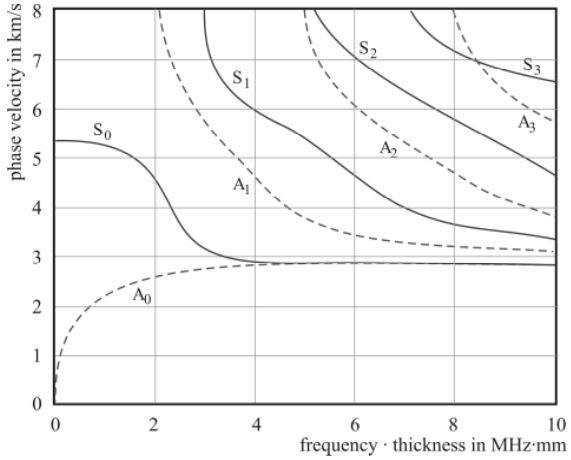

Figure 1. Dispersion diagram of an aluminum plate

The above addressed theory of wave motion in elastic solids is fundamental when the characteristics of wave propagation are used for fault detection. Faults can be considered as disturbances of an otherwise homogeneous elastic body which cause reflections, refractions and mode conversions of waves. These phenomena have to be captured by appropriate measurement techniques. Thus, a brief introduction into speckle interferometry is given in the following.

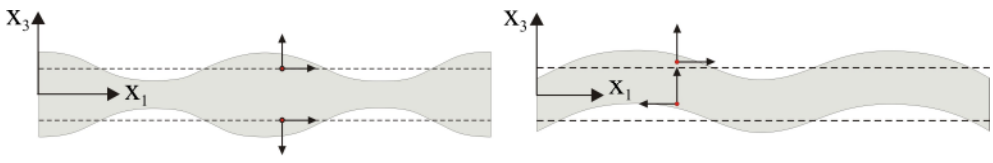

Figure 2. Fundamental lamb wave mode shapes. Left: symmetric (S_0) mode; right: antisymmetric (A_0) mode. Directions of particle movement indicated by arrows.

3. INTERFEROMETRIC MEASUREMENT TECHNIQUES

In this work, the double pulsed electronic speckle pattern interferometry (ESPI) is applied in order to investigate wave propagation in plate and shell structures. A comprehensive description of this measurement technique is given by Rastogi [9] as well as by Jones and Wykes [10].

3-1. Double pulsed Electronic Speckle Pattern Interferometry (ESPI)

The principle experimental setup for Lamb wave observation by use of speckle interferometry consists of components for the generation of coherent light, the actual interferometric setup for splitting and recombining the object illumination and the reference light as well as the data acquisition devices and components for the control of the experiment and for data post processing. Continuous or pulsed lasers are used as coherent light sources and have to be adjusted in wavelength and energy to match the requirements with reference to the specimen properties and the nature of the processes under investigation.

Speckle interferometry relies on the interference pattern which forms when an optically rough surface is illuminated by a laser beam, i.e. the object beam. The pattern which shows a granular appearance and which is called speckles is the carrier of information. The properties of the interference pattern (precisely spoken, the intensity I of any given point in the image plane) change when the test specimen undergoes rigid body motions relative to the interferometric arrangement or surface deformations. The object beam is the variable optical path of the interferometer. The second part of the laser beam, the reference light, is used for the interferometric measurement. It is directed along the non-changing optical path of the interferometric arrangement. If the reference wave is in form of another, non-changing speckle field, the interferometer uses a speckle reference wave. In the alternative case of a plane reference wavefront, it is a smooth reference wave interferometer. Both object and reference beam, are recombined to build a speckle pattern formed from the coherent addition of the speckle pattern of the scattered object illumination and the reference beam. The intensity distribution of the speckle pattern is recorded by electronic devices, e.g. CCD cameras.

Each recorded speckle image encodes in its speckle intensity distribution a single state of the object. The motions or displacements, respectively, between initial and displaced object state result in speckle intensity variations due to an interferometric phase change. Comparative analysis of the speckle intensities in subsequent interferograms yields information about the interferometric phase change of each speckle undergone from the first, initial object state to the second, i.e. displaced object state.

The interferometric phase change is the basic information and can be visualized in phase maps. They may be used for the qualitative assessment of the quantity under investigation, e.g. the displacement component under consideration is related to the gray scale value. Further computations have to be carried out for the quantitative analysis. Several parameters of the interferometer and the recording setup are necessary for these calculations.

3-2. Basic equations

The complex amplitude A_i of the object (undisplaced or undeformed state) and the reference beam at any point *(x,y)* on the image plane (CCD array) may be written as

$$A_1(x,y) = a_1(x,y)e^{i\phi_1(x,y)}$$
$$A_2(x,y) = a_2(x,y)e^{i\phi_2(x,y)} \tag{6}$$

respectively. Here, $a_i(x; y)$ is the amplitude and $\phi_i(x, y)$ is the phase of the respective beams. The intensity I_1 at any point (x, y) on the image plane is given by

$$I_1(x,y) = A_1 + A_2 + 2\sqrt{A_1 A_2}\cos\left(\phi_1(x,y) - \phi_2(x,y)\right) = I_0 + I_m \cos\psi(x,y) \tag{7}$$

with $\psi(x,y) = \phi_1(x,y) - \phi_2(x,y)$ being the phase. The sum $I_0 = A_1 + A_2$ is called background intensity and the expression $I_m = 2\sqrt{A_1 A_2}$ is known as the modulation intensity. The intensity is time invariant.

In the case of double pulsed ESPI, a displaced or deformed state results in an interferometric phase change and thus gives rise to a modified complex amplitude

$$\bar{A}_1(x,y) = a_1(x,y)e^{i\left(\phi_1(x,y)+\Delta\phi\right)} \tag{8}$$

The speckle intensity $\bar{I}_1$ of the deformed state is now computed from the amplitudes $\bar{A}_1$ and A_2 resulting in

$$\bar{I}_1(x,y) = I_0 + I_m \cos\left(\psi(x,y) + \Delta\phi\right) \tag{9}$$

The difference between the two speckle patterns which is obtained by subtracting both images produces a fringe pattern (phase map) and corresponds to the deformation field. If I_0, I_m, and ψ are assumed to be time independent and if the illumination and observation directions are kept unchanged the displacements may be computed from $\Delta\phi$.

4. EXPERIMTENAL SET-UP AND MEASUREMENT PROGRAM

In this Section, the interferometric set-up for Lamb wave observation is presented as well as the test specimens and the procedure for their excitation. Furthermore, the measurement program is specified.

4-1. Set-up for Lamb wave detection

For Lamb wave observation hardware components and software of the ESPI system DANTEC Dynamics Q600 are used. The core of the system is a customized pulsed ruby laser Lumonics HLS2 with a wavelength of $694 \cdot 10^{-9}$m. Its technical specifications are given in Table 1. The measurement control and analysis PC triggers the optical system. The minimum trigger delay is $1.2 \cdot 10^{-3}$s and accounts for the generation of the laser pulse. In order to generate a double pulse for the two exposures a Pockels cell is used. In the execution of the experiments, the pulse separation time plays an important role since the second object state is selected by this parameter. Some other settings are used for a balanced distribution of the total energy on the two pulses.

After the interferograms are captured and analyzed the interferometric phase change is computed and displayed as phase map which is a meaningful first quantitative result. Subsequent data processing allows for a visualization of the displacements in a three dimensional representation and of cuts through the deformed specimen according to a previously defined line.

quantity	specification
wavelength	$694 \cdot 10^{-9}$m
coherence length	$\approx$ 1m
energy (single pulse)	1J
pulse duration	$30 \cdot 10^{-9}$s
pulse separation time	$8 \cdot 10^{-6}\text{s} \leq \Delta t \leq 800 \cdot 10^{-6}$s
puls repetition time	4/min

Table 1. Specifications of the double pulse laser Lumonics HLS2

4-2. Test specimens and lamb wave generation

Aluminum plates (1000mm × 1000mm) of 0.5mm thickness are selected as test specimens. In a first investigation, such a plate is solely equipped in its center by a piezoelectric actuator for Lamb wave generation as described below in detail. Subsequent experiments deal with plates on which small aluminum plates (20mm × 20mm up to 40mm × 40mm) of 1.5mm thickness are adhered so that stiffness discontinuities are obtained. These small plates are fixed at various distances (200mm, 300mm, and 400mm) from the actuator location either on one side of the plate or on both sides. A further plate was equipped with circular holes of various diameters, i.e. 7mm, 15mm, and 25mm, likewise at the above mentioned distances from the actuator location. During the experiments, all the plates are supported by several wooden pins. Great care was taken to avoid wave reflections at these locations. In either case, modeling clay is attached to the edges of the plate under investigation in order to eliminate boundary reflections. These test specimens are shown in Figure 3.

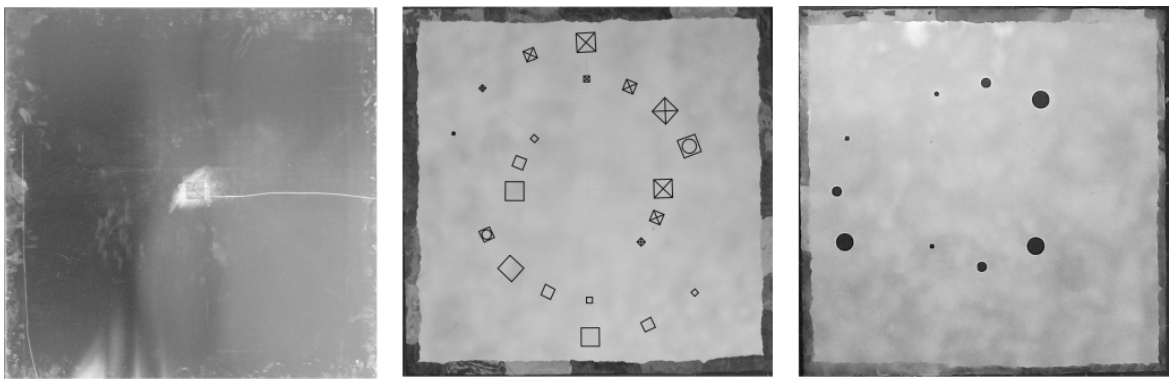

Figure 3. Plate specimens for investigation of lamb wave propagation. Left: Faultless plate with centric actuator; center: plate with stiffness discontinuities (without label: upper side; cross: lower side; circle both sides; filled: sensor); right: plate with holes.

In order to extend the investigations to real structures further experiments are made on the elevator flap of an airplane (Breguet 1150) which has not been in service. This flap is made from aluminum and shows the typical skin stringer design of a lightweight structure, cf. Figure 4. The skin is 0.5mm thick and is fixed to L-shaped stringers by rivets. Additionally, an adhesive foil is located between the stringers and the skin which is amplifying the damping capacity of this joint.

The Lamb waves are generated by two thin piezoelectric plates which are bonded with a thin layer of an insulating adhesive (Loctite 401) to one surface in the center of the plates under investigation. The flap is also equipped in this way, namely at the inner side of one skin panel. The dimensions of these actuators are 20mm × 50mm. They are driven by a frequency generator and an amplifier. The peak-to-peak signal is 290V. The amplification ensures that the amplitudes of the Lamb waves are large enough for being detected by the ESPI-system.

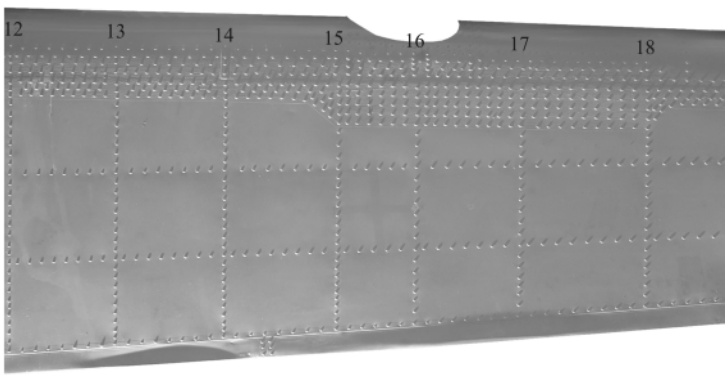

Figure 4. Riveted airplane elevator flap.

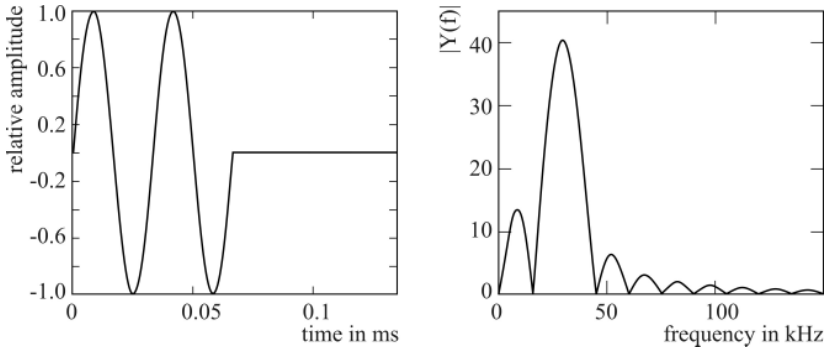

Figure 5. Actuator driving signal for Lamb wave generation. Left: time domain; right: frequency domain.

Depending on the frequency different Lamb modes can be generated as it can be seen from the dispersion diagram in Figure 2. In the following investigations, a two cycle sine burst at 30kHz is used as an excitation signal of the S_0- and the A_0-modes. The excitation signal is shown in Figure 5 in the time as well as in the frequency domain. In the frequency domain it shows significant frequencies at 8kHz and 30kHz. Higher frequencies are not considered in the following since no corresponding Lamb waves have been observed. In preceding analytical investigations and preliminary tests, this kind of signal has turned out to be advantageous with respect to the specimens and the mounted actuators.

4-3. Measurement program

The first aim of the measuring program is the visualization of symmetric and antisymmetric Lamb waves by use of the double-pulsed ESPI technique. These investigations are carried out with the faultless plate. The plausibility of the experimental results is verified by theoretical considerations. Furthermore, the investigations aim at the exposition of mode reflections and mode conversions. For that reason, subsequent experiments are performed with plates with stiffness discontinuities and holes. Finally, the experiments on the elevator flap are carried out in order to study the Lamb wave behavior at stringers and rivets.

5. RESULTS AND DISCUSSION

5-1. Faultless plate

The phase maps in Figure 6 show the propagation of the undisturbed Lamb wave in the faultless plate at consecutive points of time which are given below the respective phase maps. Here t0 denotes the beginning of the recording. The results are obtained at a pulse separation time of 8s. Some phase maps show black regions which result from a missing correlation of the underlying speckle images. The preceding wave in the front with small wave length is related to the excitation at 30kHz whereas the following wave is generated at 8kHz (best visible at t = t0 + 360µs). These excitation frequencies are related to different phase velocities of the related Lamb waves as it can be seen from the dispersion diagram in Figure 1. The spatial extension of the waves in radial direction is explained in this way and thus indicates the dispersive character of the Lamb waves. Due to the rectangular shape of the actuators the wave crests do not propagate as perfect circles.

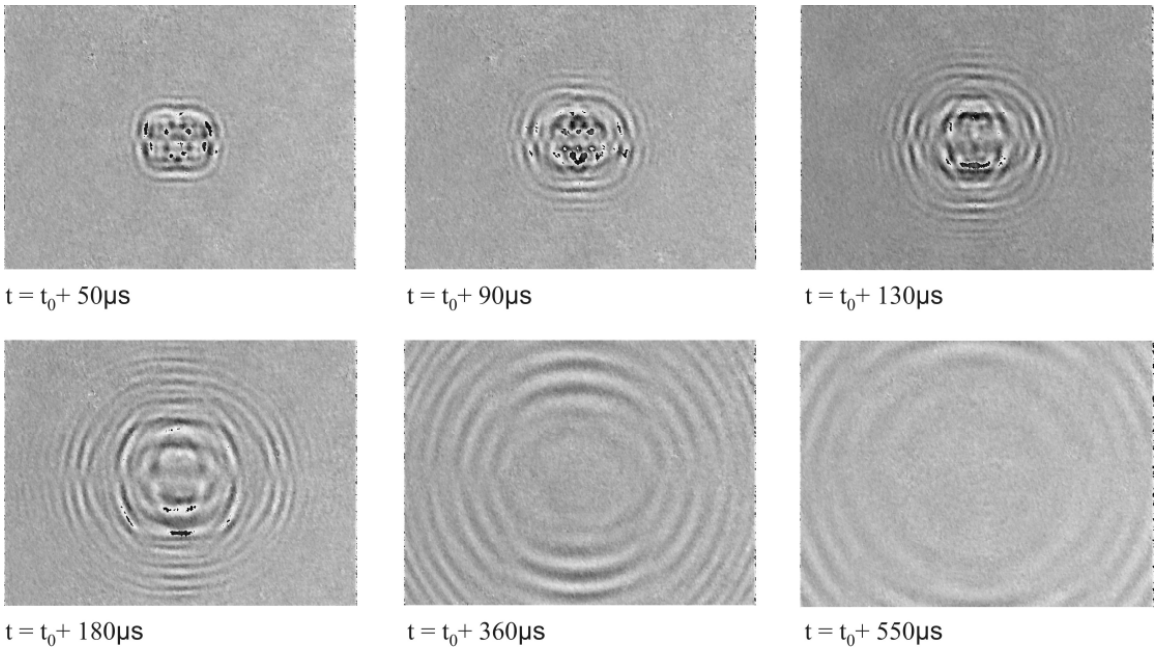

Figure 6. Propagation of the antisymmetric Lamb wave in the faultless plate. Visualization by phase maps at consecutive points of time.

Figure 7 shows the propagation of the symmetric Lamb waves by visualization of the phase maps at progressive points of time. These results were obtained at a pulse separation time of 15µs. The symmetric Lamb wave is less pronounced compared to the antisymmetric one due to its smaller amplitude. Subsequent analysis of these experimental data gives a phase velocity of 5400m/s for the symmetric and of 350m/s for the antisymmetric wave at 30kHz. The corresponding wave lengths are 185mm and 13mm, respectively. These results are in excellent agreement with accompanying analytical and numerical investigations presented by von Ende et al. [11] which yield 5375m/s and 375m/s as phase velocities of the symmetric and antisymmetric waves, respectively, and 179mm and 12.5mm as corresponding wave lengths.

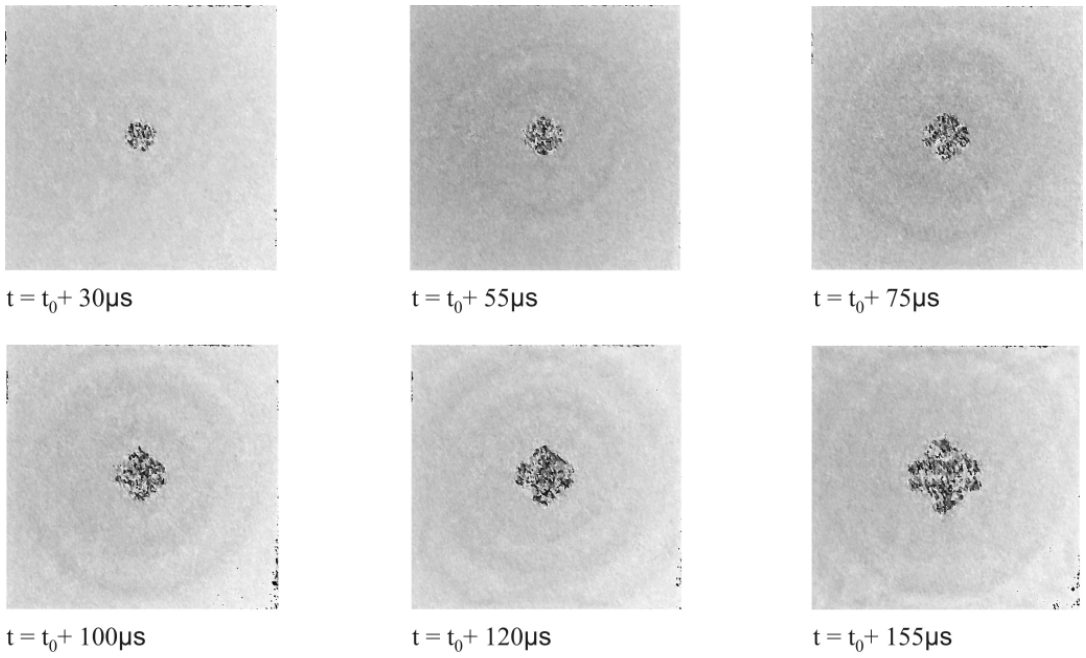

Figure 7. Propagation of the symmetric lamb wave in the faultless plate at consecutive points of time.

5-2. Plate with stiffness discontinuities and plate with holes

The subsequent investigations were concerned with the aluminum plate on which small aluminum patches were bonded acting as stiffness discontinuities, cf. Figure 3. The experiments showed that the symmetric Lamb wave is particularly suitable for the detection of the stiffness discontinuities whereas less pronounced phase maps were obtained from the antisymmetric Lamb wave. Figure 8 shows the situation at a given time in the center section of the plate. The pulse separation time is 15s. The circularly propagating symmetric Lamb wave is clearly visible. The phase map demonstrates furthermore that the symmetric Lamb waves are reflected at the stiffness discontinuities and converted into antisymmetric Lamb waves. They are easily identifiable by the shorter wave length. Thus, the difference of the wavelengths is extremely beneficial for the perceptibility of the stiffness discontinuities. This advantage becomes lost if the monitoring is based on the antisymmetric Lamb wave. All stiffness discontinuities were detected in the above-mentioned

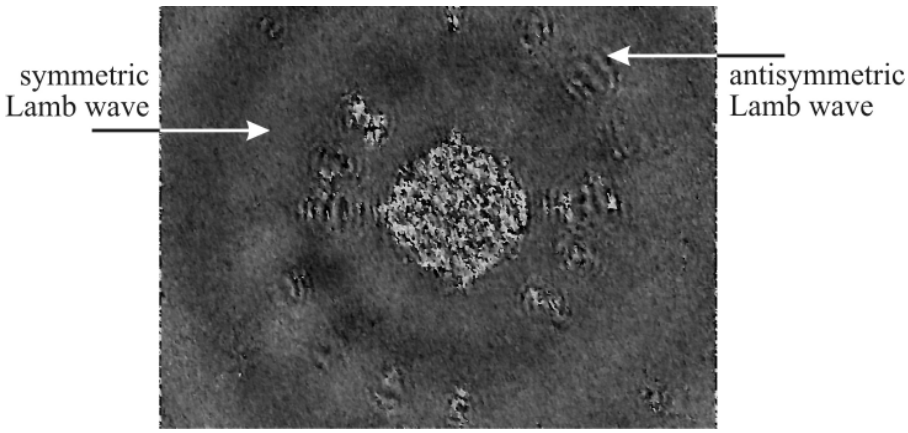

Figure 8. Phase map for visualization of symmetric Lamb waves propagating in an aluminum plate with stiffness discontinuities. Detection by Lamb waves after mode conversion.

way. Since the zoom option of the measurement system was used only the mode conversions at the two inner rings of stiffness discontinuities are visible in Figure 8. Further results which were obtained by use of other parameters in the execution of the experiments are presented by Wedel [12].

Further investigations were performed on the aluminum plate with circular holes which of course can also be considered as stiffness discontinuities. Preliminary experiments have shown that antisymmetric Lamb waves are advantageous in this case and that a frequency of 5kHz is particularly suitable. Symmetric Lamb waves move around the rather smooth boundaries of the holes without pronounced reflections and mode conversions. Figure 9 depicts an exemplary result which shows clearly the reflections and the mode conversions of the antisymmetric Lamb waves as well as their propagation around the holes. In these investigations the zoom option is also used. The aluminum plate shows another defect which has been induced by a hammer impact. The resulting local reduction of the plate thickness is clearly indicated by a disturbed Lamb wave propagation.

These experiments give rise to the question which Lamb wave, the A_0- or the S_0-wave should be used for fault detection. Figure 2 shows mode dependent movements of the individual material points of the plate structures. It may be concluded that the energy distribution of the S_0-wave is more or less uniformly distributed across the thickness whereas the surface regions transmit most of the energy in case of the A_0- wave. Since the movements of the material points interact with possible faults of the structure a defect may be detected reliably if the fault location is in the region of maximum energy. For that reason the use of the A_0- wave should be advantageous in the case of surface defects.

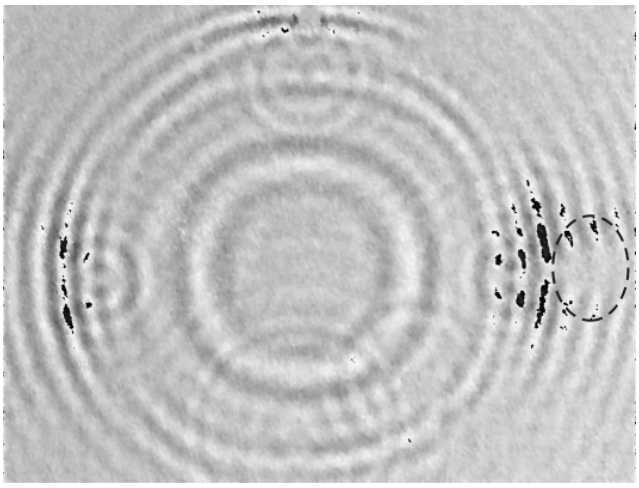

Figure 9. Phase map for visualization of antisymmetric Lamb waves propagating in an aluminum plate with holes. Detection of holes by Lamb waves after mode conversion. Dashed line marks the location of the hammer impact.

5-3. Riveted lightweight structure

The investigations on the elevator flap of the aircraft were performed in the same way as the preceding experiments on the plates. The CCD camera zoomed into the actuator equipped skin panel. One of the results is the phase map which is shown in Figure 10. The symmetric Lamb wave has reached the rivets and each of them induces antisymmetric Lamb waves which can easily be identified. These distinct patterns at the rivet locations gave the idea of loosening and removing rivets in order to find these artificial faults. In the related investigations, cf. Wedel [12], these faults could also be identified. These experiments give tentative information for ongoing work. For the structure under investigation, the symmetric Lamb waves are able to pass the stringers and to spread out over three skin panels whereas the antisymmetric one does not leave the panel in which the actuator is located. This finding may be important for future design rules of health monitoring systems.

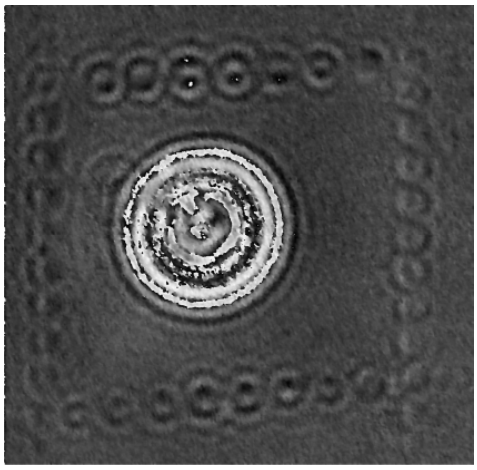

Figure 10. Phase map for visualization of the Lamb wave propagation in a lightweight structure with riveted skin stringer joints.

6. CONCLUSIONS AND OUTLOOK

The above presented experiments show clearly that the double pulsed electronic speckle interferometry (ESPI) is able to capture the displacement field of Lamb waves on the surface of thin

plates and shells. Furthermore it has been shown that this non-contact and full-field measurement technique allows for the detection of stiffness discontinuities as well as holes. Therefore, double pulsed ESPI is considered as a candidate measurement technique for further investigations on fault detection and structural health monitoring. The experiments on the riveted elevator flap encourage extending the field of possible applications to quality assurance. Another interesting finding was the detection of a partially debonded actuator which was clearly identifiable from the pattern of the generated wave. This fact is worth to be noticed since future health monitoring systems themselves have to be kept under surveillance. Further investigations will aim to detect faults not only with respect to their location but also with respect to their extent. Moreover, not only metallic but also plastic structures will be in the focus as well as fiber reinforced plastics.

ACKNOWLEDGEMENTS

The financial support of the Deutsche Forschungsgemeinschaft (DFG) is gratefully acknowledged.

REFERENCES

1. Giurgiutiu, V., “Structural health monitoring with piezoelectric wafer active sensors“, Academic Press, Burlington, MA, USA (2007).
2. Gordon, G. A. and T. D. Mast, “Wide-area imaging of ultrasonic Lamb wave fields by electronic speckle pattern interferometry“, *Proc. SPIE*, 3586:297-309 (1999).
3. Mast, T. D. and G. A. Gordon, “Quantitative flaw reconstruction from ultrasonic surface wavefields measured by electronic speckle pattern interferometry“, *IEEE Transaction on Ultrasonics, Ferroelectrics, and Frequency Control*, 48:432-444 (2001).
4. Staszewski, W. J., B. C. Lee, L. Mallet, and F. Scarpa, “Structural health monitoring using scanning laser vibrometry: I Lamb wave sensing“, *Smart Materials and Structures*, 13:251-260 (2004).
5. Barth, M., B. Köhler, and L. Schubert, “3D-visualization of Lamb waves by laser vibrometry“ , in: *Proc. 4th Europ. Workshop on Structural Health Monitoring, DEStech Publications*, 641-648 (2008).
6. Achenbach, J., “Wave propagation in elastic solids“. North Holland, Amsterdam, The Netherlands (1973).
7. Graff, K. F., “Wave motion in elastic solids“, Clarendon Press, Oxford, UK (1975).
8. von Ende, S., R. Lammering, and I. Schäfer, “Lamb Wave Generation and Propagation - Analytical Modeling and Verification -“, in: *Proc. 16th Int. Conference on Adaptive Structures and Technologies, DEStech Publications* (2008).
9. Rastogi, P. K. (Ed.), “Digital speckle pattern interferometry and related techniques“, Wiley & Sons, Chichester, UK (2001).
10. Jones, R. and C. Wykes, “Cambridge studies in modern optics 6: Holographic and speckle interferometry“, Cambridge University Press, Cambridge, UK (1989).
11. von Ende, S. and R. Lammering, “Investigation on piezoelectrically induced Lamb wave generation and propagation“, *Smart Materials and Structures*, 16:1802-1809. (2007).
12. Wedel, J., “Experimentelle Untersuchung der Wellenausbreitung nach deren Anregung durch piezoelektrische Aktoren in dünnen Flächentragwerken mit optischen Messverfahren“, Diploma Thesis, Institute of Mechanics, Helmut-Schmidt-University, Hamburg (2008).